

THE PENNSYLVANIA STATE UNIVERSITY
SCHREYER HONORS COLLEGE

DEPARTMENT OF ENGINEERING SCIENCE AND MECHANICS

LOW TEMPERATURE AND PRESSURE ELASTOMER AIDED WELDING OF GOLD
CONTACTS FOR INCREASED ELECTRONIC DEVICE MODULARITY

MICHAEL DEXHEIMER
SUMMER 2018

A thesis
submitted in partial fulfillment
of the requirements
for a baccalaureate degree
in Engineering Science
with honors in Engineering Science

Reviewed and approved* by the following:

Huanyu Cheng
Assistant Professor of Engineering Science and Mechanics
Thesis Supervisor

Charles Bakis
Distinguished Professor of Engineering Science and Mechanics
Honors Adviser

Judith A. Todd
P.B. Breneman Department Head Chair
Department of Engineering Science and Mechanics

* Signatures are on file in the Schreyer Honors College and the College of Engineering Science
and Mechanics

ABSTRACT

Low pressure and temperature welding has the ability to improve electronic device function and fabrication. Currently there are important implications in bottom-up manufacturing and advantages to stable and strong circuit interconnects. Improvements in the low pressure and temperature welding can improve device modularity and in turn device functionality. In this paper, elastomer aided gold to gold welding is investigated. Elastomer aided welding has implications in the expanding field of flexible electronic device in addition to bottom-up manufacturing. Throughout this project gold to gold elastomer aided welding is analyzed across various temperatures (100°C, 150°C, 200°C, 250°C, and 300°C) with an applied clamp pressure estimated to be 1.5kg. From these tests, it is hypothesized that elastomer aided gold welding helps to lower the critical weld temperature and pressures, and can even lead to welding under ambient conditions. Evidence of welding was reported at temperatures as low as 100°C, while the typical critical weld temperature under like pressure conditions exists at around 150°C.

TABLE OF CONTENTS

| | |
|--|-----|
| LIST OF FIGURES | iii |
| LIST OF TABLES | iv |
| ACKNOWLEDGEMENTS | v |
| Chapter 1 Introduction | 1 |
| <i>1.1 Objective</i> | 1 |
| Chapter 2 Literature Review | 2 |
| <i>2.1 Temperature and Pressure Dependence of Gold</i> | 2 |
| <i>2.2 Cold Welding</i> | 4 |
| Chapter 3 Methods | 13 |
| <i>3.1 Process and Planning</i> | 13 |
| <i>3.2 Mechanical Design Iterations</i> | 14 |
| <i>3.4 Substrate Fabrication</i> | 18 |
| <i>3.5 Selected Parameters for Measurement</i> | 20 |
| Chapter 4 Results | 21 |
| <i>4.1 Cold Welding and Peel Test Data</i> | 21 |
| <i>4.2 Clamp Applied Pressure and Final Apparatus Data</i> | 22 |
| Chapter 5 Discussion | 26 |
| <i>5.1 Cold Welding Results and Speculation</i> | 26 |
| Chapter 6 Conclusions | 31 |
| <i>6.1 Conclusions</i> | 31 |
| <i>6.2 Future Perspective</i> | 32 |
| Appendix A..... | 34 |
| BIBLIOGRAPHY | 37 |

LIST OF FIGURES

| | |
|---|----|
| Figure 1. Shear strength vs. temperature for Au- Au contacts. Ang et al 2005.(1)..... | 3 |
| Figure 2. Illustration of substrate fabrication from Ferguson et al. (2) | 5 |
| Figure 3. Capillary-force-induced cold welding of AgNWs demonstrated by Liu et al..... | 9 |
| Figure 4. Illustrations of substrate fabrication, Adrega et al. (11) | 11 |
| Figure 5. Cold welding cavity application (left), cold weld micro plotting (right)..... | 12 |
| Figure 6. Rectangular prism load cell attachment..... | 14 |
| Figure 7. Heat gun and clamps used to apply load | 16 |
| Figure 8. Final set-up for adhesion testing..... | 17 |
| Figure 9. Substrate design iterations..... | 19 |
| Figure 10. Surface changes under clamp pressure (200°C) | 22 |
| Figure 11. 50x magnification before (left) and after (right) separation | 22 |
| Figure 12. Adhesive force across temperature for clamp applied pressures..... | 23 |
| Figure 13. Measured force over elapsed time, 200°C/clamp pressure (Sample 3) | 24 |
| Figure 14. Measured force over elapsed time, 100°C/clamp pressure (Sample 1)..... | 24 |
| Figure 15. Surface results after adhesive force test for trial #3, and sample set-up (right)..... | 25 |
| Figure 16. Gold - gold broken weld SEM fractograph (1)..... | 28 |

LIST OF TABLES

| | |
|---|----|
| Table 1. Cold welding trials (Room Temperature)..... | 21 |
| Table 2. Average adhesive forces for clamp applied pressure under varying temperatures | 23 |
| Table 3. Clamp Pressure Trials 1-3 with Std. Error..... | 36 |

ACKNOWLEDGEMENTS

I want to first thank Dr. Cheng for all the help and guidance he has provided me throughout this project and throughout the entirety of the time spent in his lab. He has given me the opportunity to not only apply my coursework through research projects and discussion, but also to expand upon the tools Engineering Science has given me. I worked in an environment that allowed for creativity and constant questioning. Working in his lab fostered learning and productivity. I know that I will be using the skills that this lab has provided me as I continue my academic career over the next few years and beyond.

Secondly, I want to thank Yuyan Gao, the graduate student that closely helped me in completing this project. He has been vital in my success over the course of the past year and I have been able to learn a great deal from our working together. I know that I will take the things I learned from not only Dr. Cheng but Yuyan as well as I continue my academic career.

Chapter 1 Introduction

1.1 Objective

With a constant need for new and improved electronic device technology across a great number of fields, low temperature and pressure gold to gold welding has great potential to expand upon currently existing devices, and become something of its own. Flexible and transient electronics have recently gained popularity due to their high applicability with regard to medical device technology, and potential applications in environmentally friendly design. In addition to this expanding field, there is interest in the ability of bottom up device fabrication and effective interconnect design. With limitations in design opportunities of traditional assembly it is advantageous in size and weight to improve the ability of a vertical assembly process. It is the objective of this project to explore the possibility of elastomer aided gold to gold welding's ability to expand the existing capabilities of flexible and transient electronic devices. In addition to this it is desired to better understand gold to gold welding's possible role in bottom up fabrication and interconnect design.

Chapter 2 Literature Review

2.1 Temperature and Pressure Dependence of Gold

The temperature and pressure dependence of gold's welding abilities plays an important role with regards to its applicability across a number of fields. More specifically, these parameters help to define gold's capabilities within electronic devices. As time progresses the need and desire for multifunctional electronics increases. With that being said, across the same time the need and desire for these electronics to be compact in size and weight increases as well. Such requirements call upon three-dimensional packaging techniques (1). Such techniques allow for the device's components to be compiled vertically (1). With the incorporation of component stacking the device's compactness significantly decrease. In using a technique like this it is required that 3D interconnects are formed when building across the z-axis. These 3D interconnects can be made through gold-gold bonding, and the formation of these interconnects depends greatly on "thermal management", which is why the temperature and pressure characteristics of gold are critical when chosen as interconnect materials.

It has been seen that the critical temperature for gold-gold welding to occur is approximately 150°C (1). A measure of weld temperature and shear strength of gold to gold contacts can be seen in Figure 1. From this it can be observed that there is a linear rise in shear strength as the applied temperature of bonding is increased above and beyond the critical temperature of 150°C.

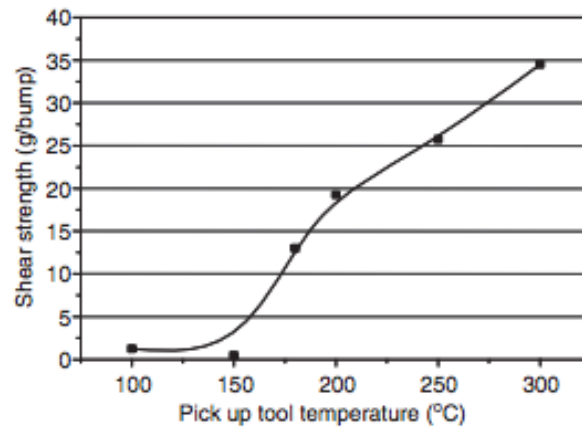


Figure 1. Shear strength vs. temperature for Au- Au contacts. Ang et al 2005.(1)

The ability to increase the strength of the gold to gold contacts near the critical temperature would greatly increase device modularity capabilities by decreasing not only the cost but also mechanical damage in fabrication and thermal damage or defects caused by the excessive heating. In order to take advantage of a technique capable of this, cold welding processes should be investigated.

2.2 Cold Welding

Cold welding techniques provide a path for increased modularity within electronic device design. Cold welding allows for the welding of metals under ambient conditions (2).

Additionally, cold welding is often found in the absence of atmosphere, especially under atomically flat conditions. There are a few proposed mechanisms of cold weld bonding. One such mechanism can be described as the breakthrough of the “brittle cover layer” (3). Such a mechanism relies on the deformation or fracture of a “work-hardened” surface layer on the metallic surface that is to be welded. Another proposed mechanism of cold welding, and most predominately discussed throughout this paper, is the is contaminant film mechanism (3). This mechanism relies on the deformation of a contaminant film layer on the desired metallic surface. Breakthrough of such a layer exposed “base” materials and allows for necessary contact and eventually welding to occur (3).

Measures are typically taken to prevent the process of cold welding from occurring, for example, under the high vacuum and high-pressure environments of space. But this phenomenon of cold welding can be taken advantage of for the purpose of device assembly (4). Ever expanding techniques and processes of device manipulation and assembly continually improve the capabilities of electronics across all fields. Cold welding techniques possess the ability to contribute to this expansion.

Historically, success in cold welding had come from the aforementioned high pressures and temperatures traditionally caused by high impact or frictional forces (2,5). Since, it has been observed that cold welding can occur under ambient conditions with the inclusion of elastomeric

supports (2). Ferguson et al., shows that polydimethylsiloxane (PDMS) can act as supportive films to aid in gold-gold welding, dramatically lowering the typically required temperature and pressure and allowing for welding under ambient conditions (2). It is hypothesized that the elastomer support layers provided an increased area of contact between the gold-gold surfaces. As seen in Figure 1, Ferguson et al. utilized a 2×10^6 nm thick layer of PDMS, a less than 5 nm layer of SiO_2 , a 2 nm layer of self-assembled monolayers (SAM), and a 20 nm layer of gold.

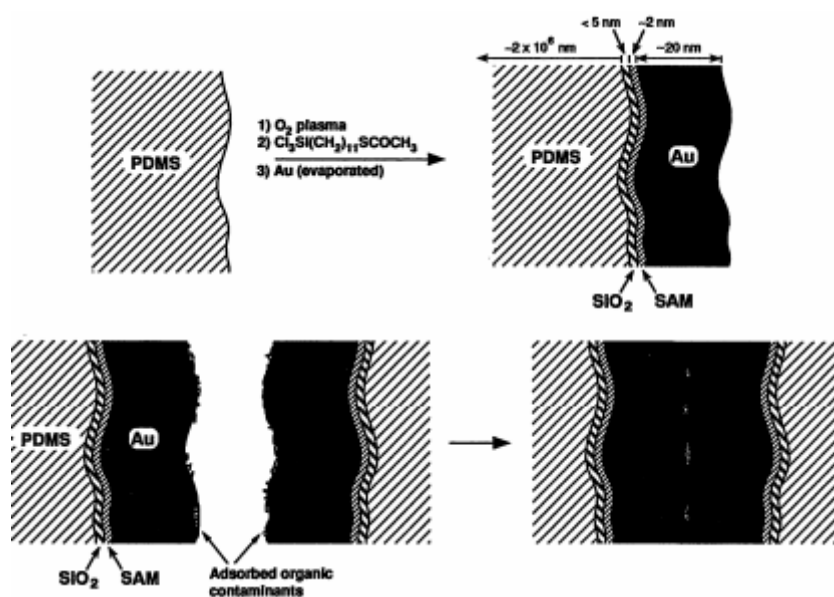


Figure 2. Illustration of substrate fabrication from Ferguson et al. (2) .

Two elastomer supported gold substrates would be brought together with an area of contact of $3.53 \times 10^{-4} \text{ cm}^2$ (2). Once adhesion was suspected to have occurred the strength of adhesion was measured using an apparatus that was able to measure the force between a semispherical

substrate and a flat sheet of substrate (6). This method allowed for the force to be calculated by measure of the radius of curvature of contact, and the applied pressure (see equations 1-3) (6).

$$(1) \quad a^3 = \left(\frac{R}{K}\right) \{P + 3\pi WR + [6\pi WRP + (3\pi WR)^2]^{0.5}\}$$

$$(2) \quad \frac{1}{K} = \left(\frac{3}{4}\right) \left\{ \frac{(1-\nu_1^2)}{E_1 + \frac{(1-\nu_2^2)}{E_2}} \right\}$$

$$(3) \quad \frac{1}{R} = \left(\frac{1}{R_1}\right) + \left(\frac{1}{R_2}\right)$$

Where, P is external load; W is the work of adhesion; R_1 and R_2 are radii of curvature of the two spheres. ν_1 , ν_2 , and E_1 , E_2 are the Poisson ratios and elastic moduli of the two substrates. From this it was calculated that the adhesive force for two elastomer supported gold films was 3.33 dyne, or 3.4 mg, for the initial contact area of $3.53 \times 10^{-4} \text{ cm}^2$ (2). It should be noted that the adhesive force for two PDMS substrates was less than 1% that of the gold to gold adhesion (2). It was further seen that in order to reproduce these results under ambient conditions at least one elastomer support was required on a single substrate. From this, Ferguson, et al. hypothesized that the elasticity of the PDMS provided a way for the gold to gold contacts to adhere to one another without being characteristically atomically flat. This was thought to be attributed to the ability of the PDMS elastomers to not only increase the contact area between the substrates but to further displace “loosely absorbed contaminants” (2).

Cold welding has continued to be tried and tested in numerous applications and experimentations. For instance, Zhang and Bay have used modeling techniques to simulate the cold-welding process (7). This type of modeling allows for a better understanding of the parameters in play concerning the cold-welding process, and allows for appropriate experimental

changes to be made. Zhang and Bay's work investigated, through simulation, the weld strength between aluminum contacts with Ni plating. It was found that the nominal weld strength (denoted as σ_B in equation 4) relative to the entire contact surface area is equal to the overlapping surface exposure (ψ) multiplied by the effective normal pressure (ρ_B) (5).

$$(4) \quad \sigma_B = \psi \rho_B$$

The effective normal pressure described by Zhang and Bay is crucial to the cold-welding process. This pressure is dependent upon the surfaces of the tested substrates. Metal surfaces with a thin layer of contamination will expose "virgin" metal layers and surfaces with ease compared to those with thicker layers of contamination. These metals with much thicker layers of contaminant films must be subject to much higher pressures. These normal pressures must reach high enough values in order to expose the "virgin" metal surface through the described layer of contamination (7).

Cold welding between gold to gold contacts has been observed not only at the macro- and microscale but also at the nanoscale. Yang Lu et al. from Rice University demonstrated that solid-state cold welding of gold-gold contacts can take place under standard conditions with induced deformation. In this case the tested gold-gold contacts were nanowires (8). This study showed "head-to-head" and "side-to-side" welding of gold wires at the nanoscale level. This was done successfully without high load and at near room temperature. Further, it was reported that there was no effect on mechanical or electrical properties of the nanowires (8). A gold and silver nanowire cold welding simulation was conducted by Pereira and Silva at the Institute of Physics "Gleb Wataghin" (9). This research further analyzed the dynamics of cold welding at the

nanoscale through molecular dynamics. This simulation confirmed the process of low temperature and pressure welding of gold to gold contacts and showed that the gold retains its crystalline FCC structure within the welded region which helps to explain the maintenance of electrical and mechanical properties of the nanowires after cold welding occurs (9).

Welding can be induced in a number of ways. As previously discussed, low temperature and pressure welding or cold welding has been demonstrated through the deformation of contamination layers, by the advantages of nanoscale contacts. But this process of cold welding can be induced through the application of capillary forces as well (10). This technique of capillary force cold welding was demonstrated in silver-silver contacts in flexible transparent electrodes (10). The way this technique was applied was by a simple two-step process which can be seen in figure 3 (10). These two steps are essentially the application of moisture and a drying step. Moisture is applied to silver nanowire (AgNW) film electrodes by use of a humidifier or even by breathing on the substrate. The applied liquid condenses near the overlaying nanowire junctions. As the water begins to evaporate a “meniscus shaped capillary bridge” is formed and draws the two nanowires in the junction together allowing for the contact necessary for cold welding to occur. Repeating this fast two-step process a small number of times allows for the established connections to further improve and new connections to be made. Repetition reduces the measured resistance and improves the electrical connections and therefore its respective

properties (10). This example shows not only a mechanism of cold welding but also a transition to the applications of cold welding through the design of the AgNW electrode device.

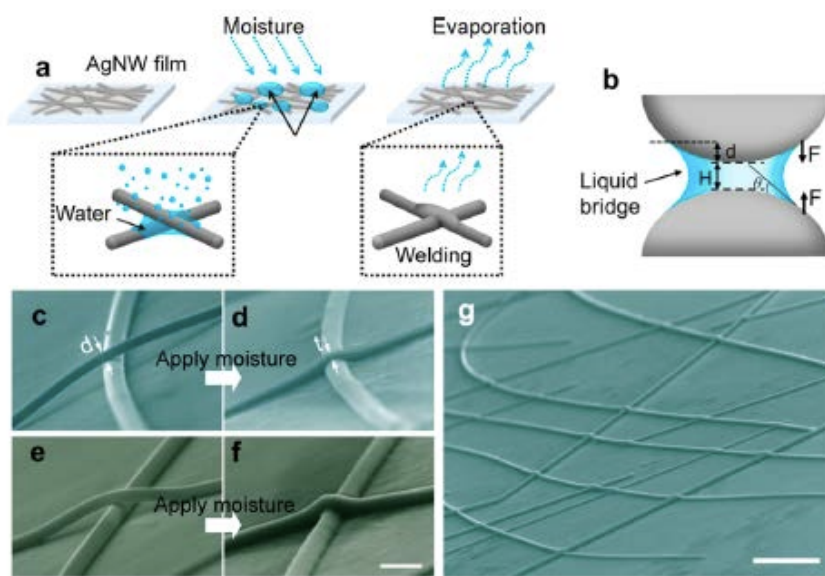


Figure 3. Capillary-force-induced cold welding of AgNWs demonstrated by Liu et al.

As previously mentioned, it has been hypothesized that low pressure and temperature welding or is capable under ambient conditions with the assistance of elastomer layers (2). This elastomer layer plays apart in not only allowing for ease of welding and strength of contact between two metal layers, but also in transient flexible electronics and further applications.

2.3 Flexible Electronics and Additional Applications

Flexible electronic devices have been on the rise within recent years. These electronic devices are capable of large deformations without loss of function, and in some cases, are capable of complete dissolution. With the recent rise in need for such environmentally friendly capabilities, the implementation of low pressure and temperature welding techniques would bring about an increase in function of such devices and expand an already quickly growing field.

One such example of the application of flexible elastomer and gold comes from a project completed by Adrega and Lacour from the University of Cambridge (11). This project focused on creating stretchable gold conductors through the utilization of PDMS elastomer (11). This is of use in display technology, stretchable circuitry, soft microelectromechanical systems (MEMS) and within the medical field for electrode applications. This study found that through photolithography fabrication, stretchable gold conductors were successfully embedded in PDMS substrate (11). Gold feature sizes as small as $10\text{ }\mu\text{m}$ were able to be produced. It was found that

the PDMS embedded conductors would remain functional (electrical properties remained intact) up to a 30% strain and radial stretching to 12% (Figure 4) (11).

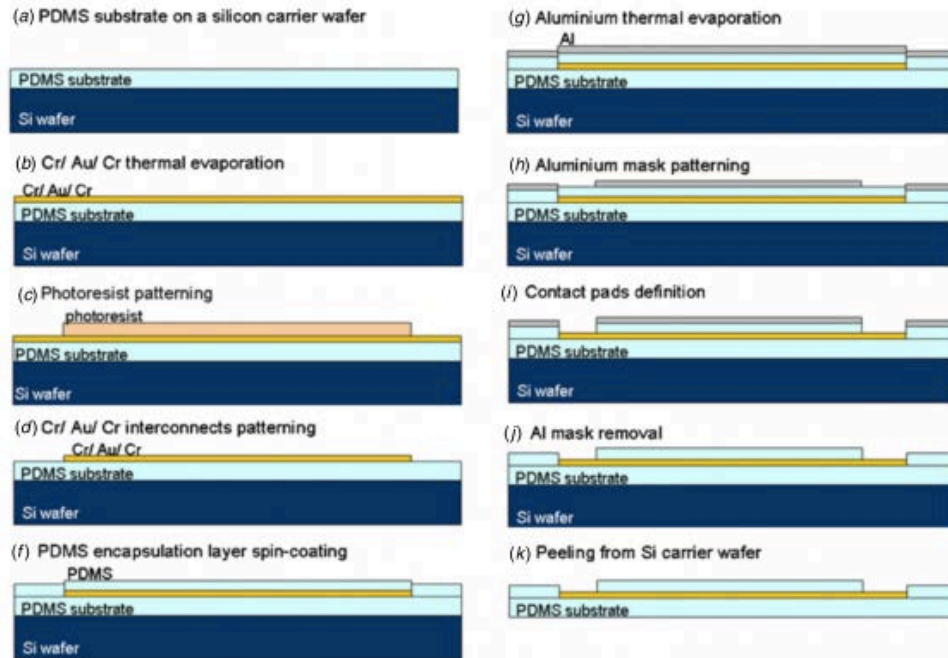


Figure 4. Illustrations of substrate fabrication, Adrega et al. (11)

Flexible electronics are not the only application of which stands to gain from improvements in cold welding. Cold welding assembly techniques have already been introduced. A technique has developed that involves the direct micro-patterning of organic electronic devices. This is done by high-pressure stamping, which induces cold welding between a metal coating on the stamp and the metal layer on the organic film (12). There are great advantages to this such as micrometer scale device patterning, fast and simple processing, and nondestructive fabrication (12). A simple schematic of the process is shown below (Figure 5 left).

Another application of cold welding is wafer attachment and sealing methods. These are used for wafer-level manufacturing, and in this case, was developed by Decharat et al., where they utilized low temperature welding for their design (13). In this study metal to metal cold welding was utilized for room-temperature sealing of micro cavities. This was able to be done by

contacting metal sealing rings, in this case gold (Figure 5). A force was applied of 2.5kN in order to bond the metal rings together and create the desired cavities. In doing this it was found that localized fractures underneath the gold existed most likely caused by the high pressures required to cold weld the cavities (13).

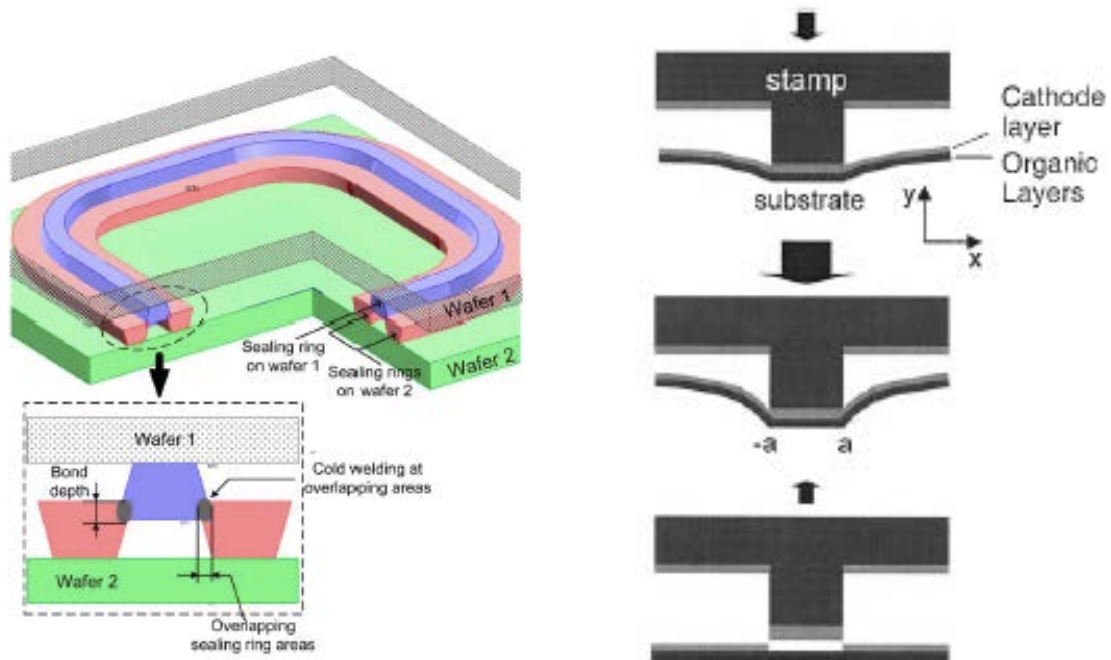


Figure 5. Cold welding cavity application (left), cold weld micro plotting (right)

The advantages of cold welding techniques expand across applications and across fields. It can be seen in areas of wafer manufacturing and flexible electronics, as well as bottom up device assembly. Cold welding serves to improve the technological capabilities across the sciences through its low pressure and temperature adhesive capabilities.

Chapter 3 Methods

3.1 Process and Planning

Designing and executing an experiment with the purpose of inducing elastomer assisted gold to gold welding required multiple mechanical setup and substrate design iterations. The goal of these experiments was to analyze the ability of gold to weld with itself under low temperatures and pressures. In order to do this, there were two significant design steps. One being the design of an apparatus capable of bringing two substrates together under pressure and various temperatures. The other being the design of the substrate. It was necessary that the substrates contained an elastomer component along with a gold component capable of remaining adhered to the selected elastomer. In the process of working towards these goals, multiple different designs were developed and executed for both the desired apparatus and substrates. The process of designing and bringing to fruition different setups and substrates yielded no results at times. But, it brought to fruition a culmination of designs and the final results of the experiment to be discussed in Chapter 4.

3.2 Mechanical Design Iterations

Throughout the experimental design process multiple experiments were performed that did not yield the necessary results. In the beginning of this process we attempted to reproduce the cold-welding results that have previously been attained (2). In order to do this a motion stage and load cell system were utilized. The motion stage and load cell devices were utilized throughout the design process and were vital tools in acquiring results. This original motion stage and load cell setup was used to bring together a two PDMS substrates. One substrate was attached, through an adhesive 1mm Ecoflex layer, to an acrylic rectangular prism (See figure 5). This rectangular piece measured a base length of ~10mm, a base width of ~5mm, and a height of ~15mm. This piece was capable of being attached to the load cell by screw and could be lowered or raised vertically onto the desired elastomer substrate at a desired rate. The motion stage apparatus was able to executed this at very slow speeds thanks to Arduino software that was used throughout this process. The slow speeds of the motion stage (~0.5mm/min) were needed in order to acquire data at a rate sufficient for the frequency of the load cell (10 Hz) to analyze.



Figure 6. Rectangular prism load cell attachment

After these cold-welding experiments were completed a new experimental design was developed. This design was a peel test. The peel test was set up very similarly to the original cold-welding design. In this case however, the substrate that would be contacted by the load cell substrate was not placed on a horizontal but instead a 45-degree plane. The load cell moved in a vertical fashion as before, but executed a peeling motion due to the 45-degree plane the substrate rested on. In doing this it was necessary to change the substrate design as well, this is to be discussed in section 3.3.

In using the previously discussed set ups, both the original cold-welding design and the 45-degree peel test design, it was necessary that changes be made to the experimental process based on the incoming results. Previously, within the original cold-welding set-up the substrate lying on the horizontal surface was not fastened or adhered to a surface. The tests that were being conducted were under low pressure and temperature (around 80 mg and room temperature conditions). As these parameters began to rise we began seeing gold to gold adhesion values capable of lifting the horizontal substrate once the motion stage began to vertically ascend. Additionally, once higher pressure and temperature values were being reached it was necessary that the apparatus have temperature protective barriers in place to ensure the device does not become thermally damaged in any way.

With these necessities in mind two new designs were executed. The first new design was the simplest set up yet. This involved a small clamp, commonly used to hold papers together, and a solder heat gun capable of reaching temperatures up to 480°C (See figure 7). The setup required that two small gold elastomer substrates be layered with gold tops contacting one another and compressed by the described clamps. The first clamp applied covered half of the exposed surface and a second clamp was applied to cover the other (See figure 7). This maximized the surface

area of which the force was applied. Finally, the heat gun was used across various lengths of time and temperatures in order to test the effects of elastomer aided gold to gold welding. The gun was set with its nozzle ~4cm from the substrates in contact. With this design, there was one final problem with its simplicity. While welding was observed, there was no way to accurately quantify the adhesive force or quality of the weld. Removing the samples from the clamps caused slight disruption in the quality of the weld as the process began to apply forces in a peeling direction due to slight adhesion observed between the metal of the clamp and the exposed elastomer surface. In order to obtain adhesive force measurements, the final force apparatus was designed.

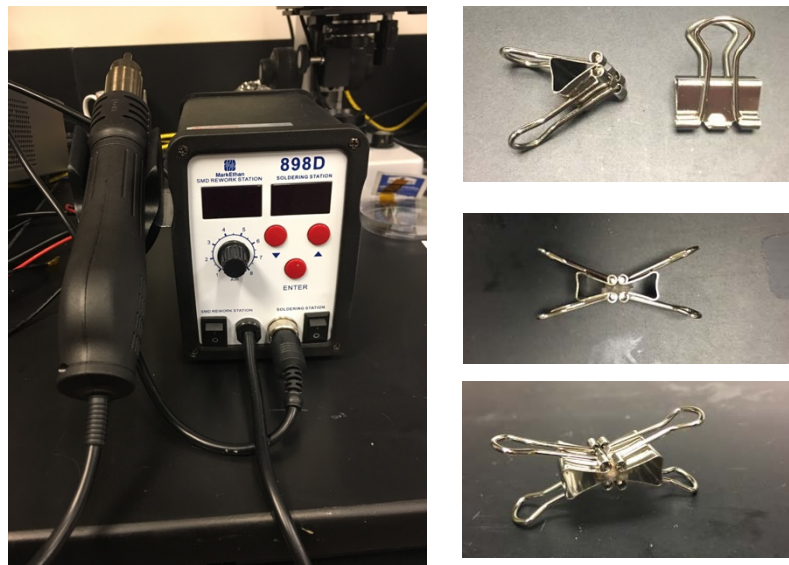


Figure 7. Heat gun and clamps used to apply load

In the final design, adhesive force measurements were able to be obtained with only slight modifications to the original cold-welding set-up. The original cold-welding set-up, as previously discussed, did not have a secure horizontal substrate. When the adhesive forces were greater than the weight of the horizontal substrate no force measurements were able to be obtained because separation had not occurred. Correcting this involved adhering the horizontal

substrate to an aluminum plate. This allowed for the substrate to be secure and for necessary force measurements to be taken. Also, as previously mentioned, it was necessary the force sensor and motion stage were protected from thermal damage. This was done by adding a thermal insulator to block the most sensitive parts of the apparatus. This final set-up varied from the original cold-welding motion stage set-up in one final way. Instead of the force sensor moving in a vertical direction, it was stationary. In order to contact the substrate, a platform located below the stationary force sensor moved vertically by using the previously described motion stage.

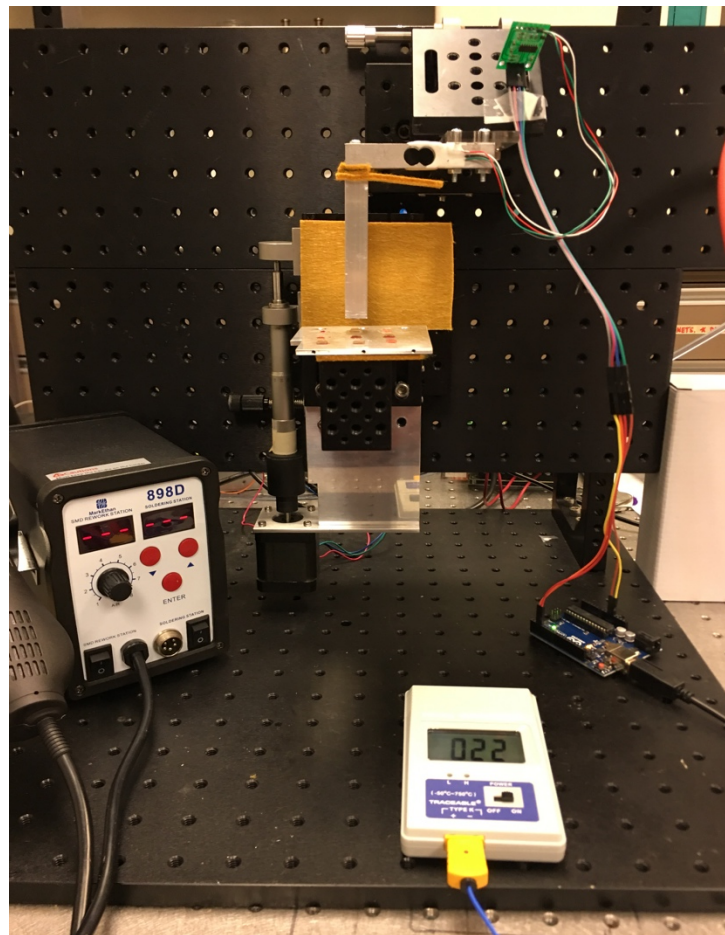


Figure 8. Final set-up for adhesion testing.

3.4 Substrate Fabrication

Much like the various design iterations involved with the mechanical motion stage set-up, there were a number of iterations involved throughout the fabrication of the elastomer substrates for testing. The first design iteration for the motion stage apparatus was the original cold-welding test. With this a few different substrates were designed. In each of the designs that were used throughout the experiments PDMS 184 was utilized. The PDMS, or polydimethylsiloxane, was made through a simple 2 step process. This process consisted of adding two mixtures, A and B, of Solaris PDMS in proportions of 10:1 and letting cure for 24 hours. At the end of this 24hrs the PDMS substrate was ready to be manipulated and the various substrate designs were fabricated.

The first design was most similar to the final iteration. This substrate was a layer of PDMS followed by 10 nm of titanium and then a 20 nm layer of gold. These metal layers were added by electron-beam or e-beam deposition. Titanium was added in this case to help support the typically weak adhesion of gold and PDMS elastomer. Variations in this design were taken on in the cold welding experimental process. As results came in describing the interaction between two planar substrates, it was decided that a spherical substrate would be fabricated. In this case, the spherical substrate was created by pouring a layer of uncured PDMS over aluminum beads. These beads had a diameter of ~7mm and were then glued to the aforementioned acrylic rectangular prism in order to manipulate its displacement with the load cell. The next design that was taken on was that of the peel test. For this design, a long substrate was needed in order to have a substantial peeling over a more significant distance. This was fabricated by use of a 3D printed mold. This mold allowed for a longer sample of PDMS to be cured, with a desired pattern. The final substrate design most closely resembles the original cold-

welding substrate. In this case however, there is one difference. Instead of using an e-beam deposited layer of gold at 20 nm, this layer was raised to 50 nm.

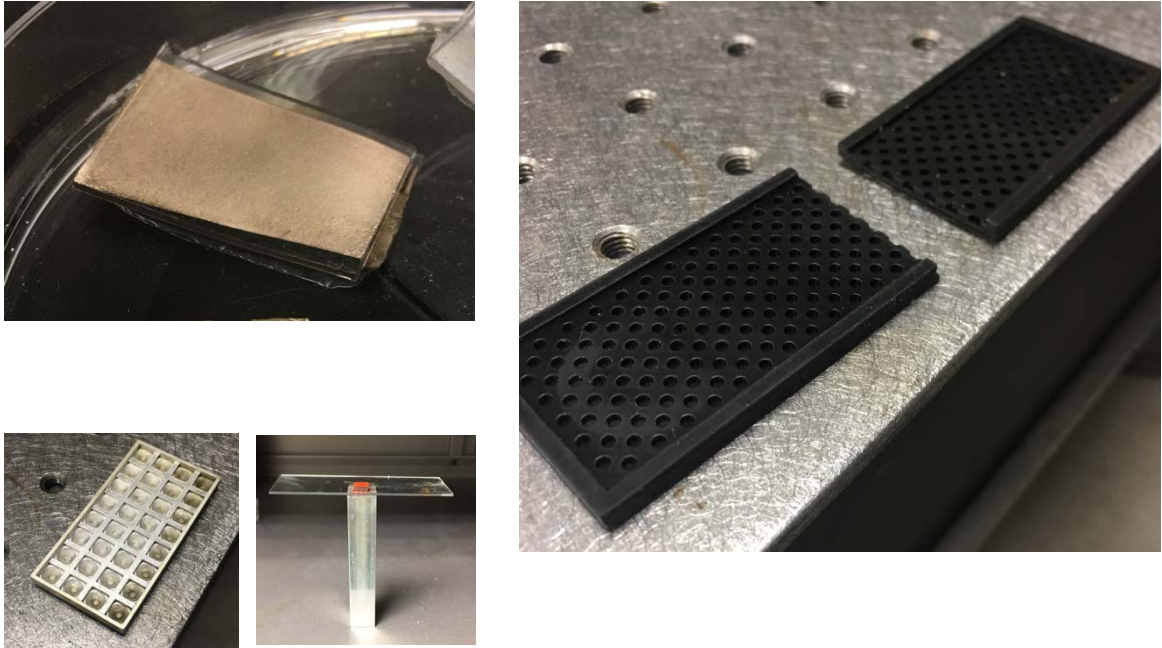


Figure 9. Substrate design iterations

3.5 Selected Parameters for Measurement

Once the final apparatus set up and substrate fabrication method was established it was necessary that parameters for measure be selected. In order to test if the addition of an elastomer substrate effected the weld quality across temperature and pressure, it was clear that the experiment would need to be conducted across temperatures and pressures comparable to those found in literature. The temperature values of 100°C, 150°C, 200°C, 250°C, and 300°C were selected as it was previously found that the minimum effective temperature to induce adhesion of gold to gold contacts started at 150°C. Further, in order to induce welding between the gold contact points of our substrate, pressure was applied to samples by a simple clamp. The applied pressure of these clamps was estimated to be around 1.5kg. This estimated pressure was applied across all samples measured in the final design. Finally, as a measure of weld quality or adhesive strength, the adhesive force of the temperature and pressure induced connections was measured by way of the final apparatus design.

Having gone through these motion stage design and substrate fabrication iterations the following results were obtained.

Chapter 4 Results

4.1 Cold Welding and Peel Test Data

Throughout the process of collecting cold welding results with the original cold-welding apparatus, results were inconsistent. Contacting two 5mm by 5mm PDMS/Ti/Au substrates under room temperature and low pressures (20g to 75g) brought about small adhesive measurements (See table 1). These unpredictable results became typical under the described conditions. The peel test measurements were conducted in order to ensure the adhesion of PDMS was within expected literature values. From these trials, it was found that similar inconsistent/unpredictable results were collected. There was no reproducibility under the presented conditions (More on this in Chapter 5).

Table 1. Cold welding trials (Room Temperature)

| Trial Number | Applied Force (g) | Adhesive Force (g) |
|--------------|-------------------|--------------------|
| 1 | 21.96 | 0.51 |
| 2 | 41.52 | 1.43 |
| 3 | 71.69 | 0.65 |
| 4 | 73.50 | 0.13 |
| 5 | 75.55 | 0.25 |
| 6 | 74.40 | 0.14 |

4.2 Clamp Applied Pressure and Final Apparatus Data

Because of the inconsistency found in the results of the cold-welding analysis, the next step was to increase pressure and temperature to induce adhesion between the tested gold to gold contacts. The first step in doing this was the application of the clamp applied pressure technique. From this, changes in the surface of the separated substrates show possible signs of adhesion. Immediately after exposure to clamp pressure and increased temperatures (200°C), changes on the surface of the substrate are evident (See figure 10). Upon further investigation, these surface changes can be seen under magnification (See figure 11).

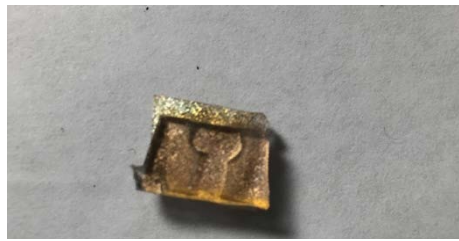


Figure 10. Surface changes under clamp pressure (200°C)

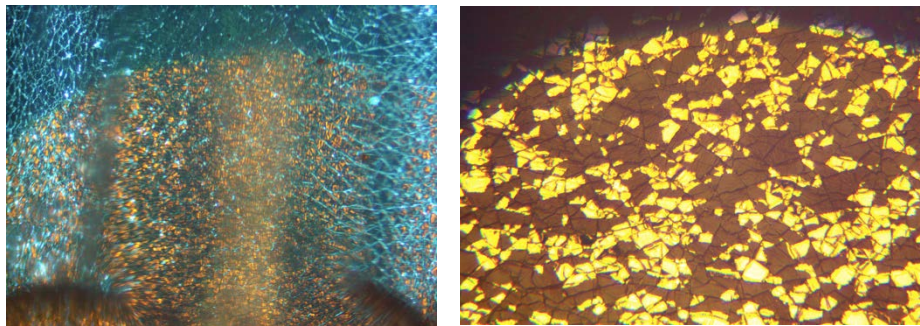


Figure 11. 50x magnification before (left) and after (right) separation

The next step in this process was to incorporate the motion stage apparatus (figure 8) in order to gather quantitative data regarding the clamp applied pressure welding thought to have been observed in figures 10 and 11. In order to do this multiple samples were run under various

temperatures (100°C, 150°C, 200°C, 250°C, and 300°C). The simple clamp pressure method was used for each sample. Additionally, a temperature exposure time of 5 minutes was used. Under these conditions the surface changes seen in figures 9 and 10 were induced and the following measurements were obtained.

Table 2. Average adhesive forces for clamp applied pressure under varying temperatures

| Trial Number | Temperature (°C) | Applied Force (kg) | Avg. Adhesive Force (g) |
|--------------|------------------|------------------------|-------------------------|
| 1a | 100 | ~1.5 or clamp pressure | 55 |
| 2a | 150 | ~1.5 or clamp pressure | 86 |
| 3a | 200 | ~1.5 or clamp pressure | 130 |
| 4a | 250 | ~1.5 or clamp pressure | 119 |
| 5a | 300 | ~1.5 or clamp pressure | 126 |

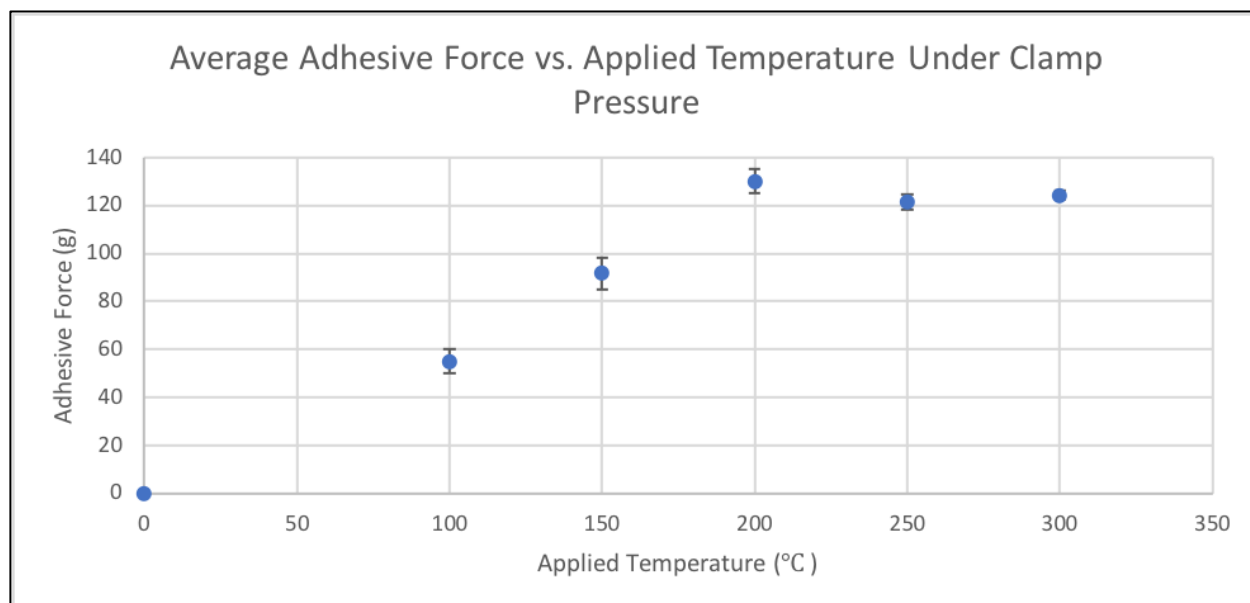


Figure 12. Adhesive force across temperature for clamp applied pressures

Specifically looking at the results of the adhesion test show an applied force (negative), followed by an adhesive force (positive peak), then followed by separation (trail off to zero force). This negative applied force is done to ensure the sample set-up in figure 16 (right) makes contact with a planar surface adhesive. This ensures that when the positive load is applied to separate the welded sample, the substrate will not become disconnected from the horizontal surface and skew the results. Typically, an applied force of ~100 g was sufficient in adhering the glass slide to the surface.

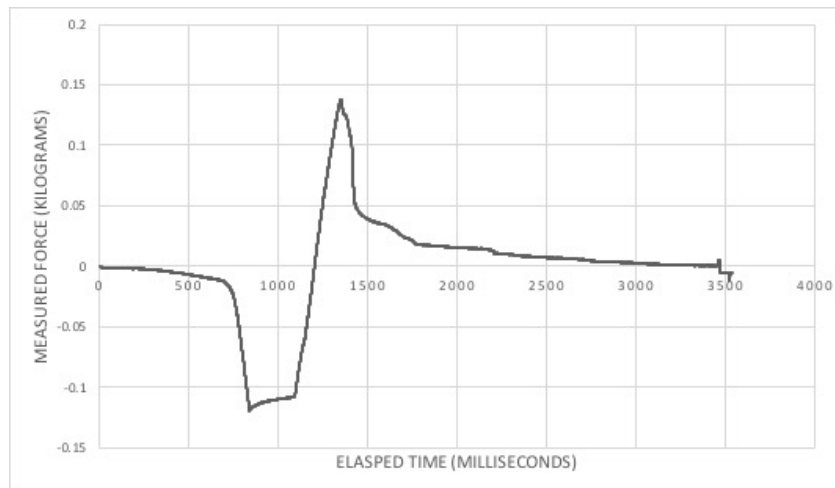


Figure 13. Measured force over elapsed time, 200°C/clamp pressure (Sample 3)

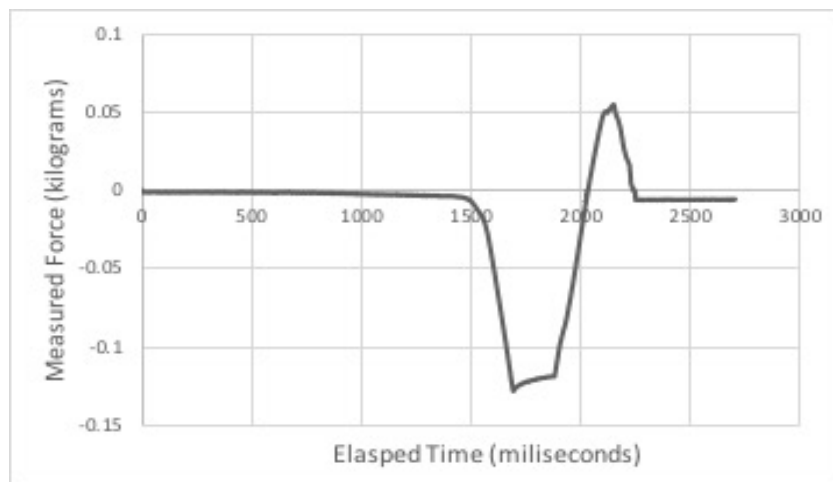


Figure 14. Measured force over elapsed time, 100°C/clamp pressure (Sample 1)

It can be seen that each sample displayed the same surface distortions, seemingly outlining the area of which the clamp's force was applied (See figure 15). These distortions were not evident in samples under pressure only, or strictly temperature. They only appeared under combinations of both clamp pressure and applied temperature.

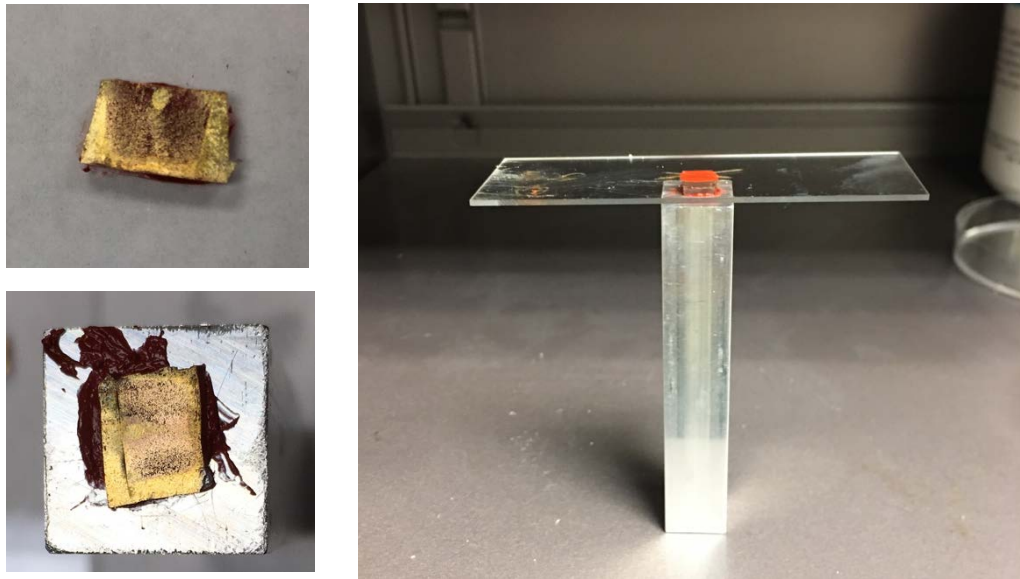


Figure 15. Surface results after adhesive force test for trial #3, and sample set-up (right)

The results of this experiment showed substantial adhesion under temperatures and pressures both quantitatively and qualitatively. The surface distortions allow one to observe the effects of applied heating under pressure, and in addition to this, considerable adhesive force was measured using the motion stage apparatus. From these results, the following discussion can take place.

Chapter 5 Discussion

5.1 Cold Welding Results and Speculation

As previously stated, the cold-welding results gained from the “original cold-welding set-up” did not exhibit any apparent trends. There were no signs of adhesion qualitatively or quantitatively. While some very slight positive adhesion values were obtained, they were not consistent or repeatable. Further, the values that were obtained were not outside of the noise threshold that was observed with the load cell in use. The maximum load that can be applied to the load cell in the original cold-welding set-up was 100 grams. It was found through repeated use that the cell was sensitive to nearly 0.02g to 0.05g with noise readings sometimes as high as +/- (0.07g to 0.15g). The inconsistency of these measurements in combination with the very unpredictable fluctuations in readings made for unreliable collections. It is possible that a more sensitive force sensor would have been able to return results indicative of slight adhesion. It can be seen from literature that with a surface area of $3.53 \times 10^{-4} \text{ cm}^2$ that a pull off force of 3.33 dyne can be seen under small pressures and ambient conditions (2). These values involve measuring force values of 3.33 dyne or 3.4 mg. The surface contact area in our experiment was around 0.25 cm^2 . With a contact area this large, is it expected that a pull off or adhesive force of around 1.90g is to be measured. This value is obtained through the scaling of the results from 1991 (2). These values are not reliably measureable while using the described load cell. Further, the relationship between the contact surface area and expected adhesive force needs to be investigated further (see chapter 6).

5.2 Elastomer Aided Gold to Gold Welding

After completing the experiments under clamp pressure and various temperatures there were some considerable signs that welding was achieved. The first sign to come to attention was the disruptions on the surface of the heat treated and clamp pressure applied samples. These substrates indicated that a significant change had occurred. These surface disruptions or deformations were not present in samples treated with either just the clamp pressure, or just temperature. In addition to this, samples treated with both clamp pressure and temperature were able to hold the force of their own weight immediately after treatment while the substrates treated with one parameter were unstable or unable to hold its own weight entirely. With this being said, PDMS to PDMS control samples were treated under temperature and pressure. In doing this no adhesive measurement was able to be made. This can be attributed to the fact that the PDMS's contact with the clamp after applying pressure was strong enough to disrupt and sometimes break whatever adhesive force may have been present between the two PDMS substrates. This allows for the conclusion to be made that the adhesive measurements gathered from gold to gold contact welding is attributed to the gold contact and not PDMS.

The described surface disturbances can be seen with the naked eye, as shown in figure 9. In addition to this, when observing under 50x magnification (as seen in figure 10), the deformations can again be seen only with more detail. An outline of the clamp's surface can be seen with several disturbances at its outermost edges (figure 10 left). When looking at these magnified images after separation of the treated samples (figure 10 right), it can be seen that a distinct pattern emerges. It appears as if though there are dark areas mixed in with the more transparent gold areas. This could be indicative of a transfer of material, which could also be

thought of as a “breaking” of the weld. Under Scanning Electron Microscope (SEM) fractographs it can be seen that gold to gold welds when broken will not remove from one another cleanly, as if they were two pieces of adhesive tape stuck together, but will instead break and appear to crumble. This idea can be seen in an image taken from Ang et al. (see figure below) (2) . The darker spots on the magnified image (figure 10 right) could be material taken from its partner substrate, while the lighter gold regions the opposite.

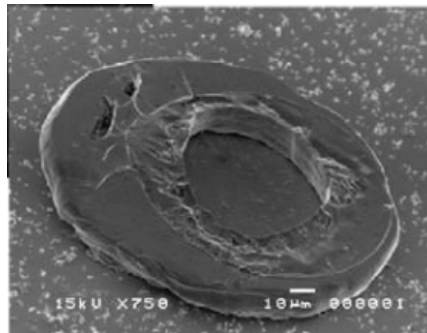


Figure 16. Gold - gold broken weld SEM fractograph (1)

The qualitative results of the clamp pressure test indicate significant adhesion has occurred between the two gold contacts. When analyzing the quantitative results similar conclusions can be made. As seen in Table 2 and Figure 11, strong gold to gold adhesion begins to appear at around 150°C and begins to taper off or plateau in adhesion strength at 200°C and beyond. These findings are consistent with literature (1). It is most commonly understood that the minimum temperature for significant gold to gold welding is 150°C. With that being said, in looking again at Table 2 and Figure 11, it can be seen that an adhesive force of 55g was found for samples treated under clamp pressure (~1.5kg) and 100°C. Looking back to Figure 1, it can be seen that samples treated at 100°C exhibited almost zero shear strength and almost the same

can be said at 150°C (1). While an adhesive force was measured for the samples in this project, these adhesive force values appeared at 100°C and were prominent at 150°C. This is different in that while welding is known to begin at 150°C, this is thought of as a “minimum” temperature. Because there is evidence of welding at these lower temperatures, as shown in Table 2, it can be hypothesized that the elastomer is aiding in the adhesion of gold to gold. It is possible that, as discussed by Ferguson et al., the elastomer substrate aids in the adhesion of gold to gold by increasing the surface area in contact (2). If this is the case elastomer aided welding could play an important role in bottom up device fabrication.

It should further be discussed that throughout the process of the project there was great difficulty reproducing welding results. This was true even with samples treated with clamp pressure and high temperatures. The welding of gold to gold contacts relies heavily on the ability of the gold contact surfaces to break through the “contamination layers” on either surface to expose virgin layers of bondable gold (7). While gold is not known to be oxidized, and for these reasons is a good substrate for ambient condition tests, contamination on the surface can build over time (11). Once cleaning protocols were applied to our sample preparation more consistent results were obtained for substrates treated under clamp pressure and applied heat. Cleaning the samples with isopropyl alcohol helped to rid the surface of contaminants to an extent, and therefore allow for more consistent results to be obtained.

Another important note to be made is that the pressure applied to the samples throughout this project was done through the described clamp. This was done for two reasons. The first reason is that we were unable to observe an adhesive force across samples with pressure applied through the motion stage. This could be caused by a difference in contact areas between the samples whose pressure was applied through the motion stage and those of the clamps. From

looking at figure 10 and figure 15 the contact area can be estimated by the clamp applied pressure. This can be done by assuming the observable deformations are the contact areas. In doing this the contact area can be estimated between $7.0 \times 10^{-6} \text{ m}^2$ and $1.2 \times 10^{-5} \text{ m}^2$. From this, using the estimated applied clamp weight of 1.5kg, the applied clamp pressures can be estimated between 1.2MPa and 2.1MPa. The uniform pressure applied by the motion stage across the entire sample area is equal to 0.74 MPa for a 5mm x 4mm sample. It can be seen that the estimated clamp pressure is significantly greater than that of the motion stage. The second reason the clamp pressure was applied is because it is a great test for our desired application. It is of great interest to be able to easily make electrical connects for devices modularity. In much the same way that the cold welding induced by capillary action was able to create electrical contacts through a mechanism as simple as breathing on a device (10), it is of great interest to be able to apply a simple clamp mechanism like the one demonstrated in this project to create necessary electrical connections.

Chapter 6 Conclusions

6.1 Conclusions

From this experiment, significant gold to gold welding evidence has been shown. Cold welding was not reproducible under these current experimental conditions. This may have been attributed to a lack of load cell measurement sensitivity. While cold welding was not reproducible, there is some evidence that low pressure and temperature gold to gold welding could have occurred. It has been shown that elastomer aided welding in this case demonstrated significant adhesion under lower than expected temperatures. Starting as low as 100°C and becoming prominent at 150°C, the adhesion strength of the substrate contacts was strong. In addition to these results it was found that under clamp pressure the adhesive force of the gold to gold substrates began to plateau or reach a maximum value at around 200°C. Further, through this experimental process there was qualitative evidence of adhesion in addition to the quantitative evidence. It was observed that under clamp conditions and applied temperature that the surface of the treated samples began to distort in a way that resembled the contact area of the applied clamp force. This was only the case when both variables were present. No distortion or disturbances were observed under clamp pressure or temperature alone.

6.2 Future Perspective

In the future, there are improvements that can be made to the current experimental design in search for the effects of elastomer aided low pressure and temperature gold to gold welding. There are also many additions to be made to better understand and confirm the proposed ideas and hypothesis in this project.

In order improve the data collection of the original cold welding experiment a force sensor capable of reliably recording forces in the milligram range should be sought after. This would allow for the confirmation of adhesion, or if no adhesion exists, it would indicate a different source of experimental error is present. In addition to this, experiments should be conducted to better understand the relationship between cold welding adhesive strength and the contact area between substrates. This would help to explain the values obtained under cold welding conditions through this project, and beyond.

With respect to the many additions that can be made to better understand and confirm the proposed ideas in this project, there are many parameters and samples that could be added to help clear up, and bring more confidence to the hypotheses present. For instance, it would be greatly beneficial to test rigid gold to gold welding against the elastomer aided gold to gold welding seen throughout this project. This would help to directly understand if the elastomer is significantly aiding in the adhesive force across lower temperatures and pressures. Additionally, lower temperatures can be tested to further understand just how different the welding of gold to gold behaves under elastomer assisted conditions. Further evidence for the support of gold to gold welding can be found in SEM imaging. In the future, samples should be analyzed under the SEM in order to directly compare to the presented literature in this project (1). Another parameter vital in testing the elastomer's significance in gold to gold welding would be the

PDMS bending stiffness and modulus of elasticity. By manipulating the type of PDMS used and the ratio of mixtures, the effect of the material properties of PDMS on the gold to gold welding adhesive values would be better understood. Finally, it would be greatly beneficial to incorporate an application of pressure into the motion stage apparatus. Currently, pressure is applied by clamp. This clamp pressure is strong and intimately related to the desired applications of the project, but imprecise and estimated. Incorporating pressure controlled by the motion stage would bring about a new level of precision and allow for adhesive strengths to be tested across a number of pressures as well as temperature.

Appendix A

Arduino Load Cell Code:

```

#define HIGHFREQUENCY 4
#define DOUT 3
#define CLK 2

HX711 scale(DOUT, CLK);

float calibration_factor = 215000; //-36 worked for my 0.5N max scale setup
unsigned long time;
void setup() {
  Serial.begin(9600);
  Serial.println("HX711 calibration sketch");
  Serial.println("Remove all weight from scale");
  Serial.println("After readings begin, place known weight on scale");
  Serial.println("Press + or a to increase calibration factor");
  Serial.println("Press - or z to decrease calibration factor");
  pinMode(HIGHFREQUENCY,OUTPUT);
  digitalWrite(HIGHFREQUENCY,HIGH);

  scale.set_scale();
  scale.tare(); //Reset the scale to 0
  long zero_factor = scale.read_average(); //Get a baseline reading
  Serial.print("Zero factor: "); //This can be used to remove the need to tare the scale.
  Useful in permanent scale projects.
  Serial.println(zero_factor);
}

void loop() {
  digitalWrite(HIGHFREQUENCY,HIGH);
  scale.set_scale(calibration_factor); //Adjust to this calibration factor

  Serial.print(" Time: ");
  time = millis();
  //prints time since program started
  Serial.print(time);
  Serial.print(" ms ");

  Serial.print("Loading: ");
  Serial.print(scale.get_units(), 6);
  Serial.print(" kg"); //Change this to kg and re-adjust the calibration factor if you follow
  SI units like a sane person

```



```

Serial.print(" calibration_factor: ");
Serial.print(calibration_factor);
Serial.println();
if (Serial.available())
{
    char temp = Serial.read();
    if(temp == '+' || temp == 'a')
        calibration_factor += 1000;
    else if(temp == '-' || temp == 'z')
        calibration_factor -= 1000;
}
}

```

Arduino Motion Stage Code:

```
#include <Stepper.h>
```

```

const int steps=400*2*4; //stepsPerRevolution =400*2*4;change this to fit the number of steps
per revolution,2 comes frm 0.9degree, 4comes from 4 steps as a loop
// initialize the stepper library on pins 8 through 11:
// pay attention: exchange channel 9 and 10 due to stepper model digital sequence.
Stepper myStepper(steps, 8, 10, 9, 11);

```

```

const int speed=180;
String readString;
void setup() {
    // initialize the serial port:
    myStepper.setSpeed(speed);

    Serial.begin(9600);
    Serial.println("Stepper motor control system");
    Serial.println("Input steps number:");
}

```

```

void loop() {

    while (Serial.available()) {
        char c = Serial.read(); //gets one byte from serial buffer
        readString += c; //makes the string readString
        delay(20); //slow looping to allow buffer to fill with next character
    }
}

```

```

if (readString.length() >0) {
  Serial.println(readString); //so you can see the captured string
  int n = readString.toInt(); //convert readString into a number

  myStepper.step(n);

  readString=""; //empty for next input
}
}

```

Table 3. Clamp Pressure Trials 1-3 with Std. Error

| Temperature | Pressure | Trial #1 Force | Trial #2 Force | Trial #3 Force | Avg. Force | Std. Deviation | Std. Error |
|-------------|----------|-------------------|-------------------|-------------------|---------------|-------------------|---------------|
| 100°C | ~1.5kg | 55g | 50g | 60g | 55g | 5.0g | 2.9g |
| 150°C | ~1.5kg | 86g | 90g | 99g | 91.7g | 6.7g | 3.8g |
| 200°C | ~1.5kg | 130g | 135g | 125g | 130g | 5.0g | 2.9g |
| 250°C | ~1.5kg | 119g | 125g | 120g | 121.3g | 3.2g | 1.9g |
| 300°C | ~1.5kg | 126g | 125g | 122g | 124.3g | 2.08g | 1.2g |

BIBLIOGRAPHY

- (1) Ang, X. F., Zhang, G. G., Wei, J., Chen, Z., & Wong, C. C. (2006). Temperature and pressure dependence in thermocompression gold stud bonding. *Thin Solid Films*, 504(1–2), 379–383. <http://doi.org/10.1016/j.tsf.2005.09.071>

- (2) Ferguson, G. S., Chaudhury, M. K., Sigal, G. B., & George, M. (2016). Contact Adhesion of Thin Gold Films on Elastomeric Supports : Cold Welding Under Ambient Conditions Published by : American Association for the Advancement of Science Stable URL : <http://www.jstor.org/stable/2879122> JSTOR is a not-for-profit service that , 253(5021), 776–778.

- (3) Bay, N. (1983). Mechanisms Producing Metallic Bonds in Cold Welding. *Welding Research Supplement*, 62, 137–142.

- (4) Santos, L. V., Trava-Airoldi, V. J., Corat, E. J., Nogueira, J., & Leite, N. F. (2006). DLC cold welding prevention films on a Ti6Al4V alloy for space applications. *Surface and Coatings Technology*, 200(8), 2587–2593. <http://doi.org/10.1016/j.surfcoat.2005.08.151>

- (5) Zhang, W. Y., Ferguson, G. S., & Tatic-Lucic, S. (2004). Elastomer-supported cold welding for room temperature wafer-level bonding. *17th IEEE International Conference on Micro Electro Mechanical Systems. Maastricht MEMS 2004 Technical Digest*, 2(c), 2–5. <http://doi.org/10.1109/MEMS.2004.1290691>

- (6) Chaudhury, M. K., & Whitesides, G. M. (1991). Direct Measurement of Interfacial Interactions between Semispherical Lenses and Flat Sheets of Poly(dimethylsiloxane) and Their Chemical Derivatives. *Langmuir*, 7(5), 1013–1025. <http://doi.org/10.1021/la00053a033>

- (7) Zhang, W., & Bay, N. (1997). Cold welding - Theoretical modeling of the weld formation. *Welding Journal*, 76(10), S417–S420.

- (8) Lu, Y., Huang, J. Y., Wang, C., Sun, S., & Lou, J. (2010). Cold welding of ultrathin gold nanowires. *Nature Nanotechnology*, 5(3), 218–224. <http://doi.org/10.1038/NNANO.2010.4>

- (9) Pereira, Z. S., & Da Silva, E. Z. (2011). Cold welding of gold and silver nanowires: A molecular dynamics study. *Journal of Physical Chemistry C*, 115(46), 22870–22876. <http://doi.org/10.1021/jp207842v>

- (10) Liu, Y., Zhang, J., Gao, H., Wang, Y., Liu, Q., Huang, S., ... Ren, Z. (2017). Capillary-Force-Induced Cold Welding in Silver-Nanowire-Based Flexible Transparent Electrodes. *Nano Letters*, 17(2), 1090–1096. <http://doi.org/10.1021/acs.nanolett.6b04613>
- (11) Mamin, H. J., Guethner, P. H., & Rugar, D. (1990). Atomic Emission from a Gold Scanning-Tunneling-Microscope Tip. *Physical Review Letters*, 65(19), 2418–2422. <http://doi.org/http://dx.doi.org/10.1103/PhysRevLett.65.2418>
- (12) Kim, C., Kim, C., Burrows, P. E., & Forrest, S. R. (2010). Micropatterning of Organic Electronic Devices by, 831(2000), 10–13. <http://doi.org/10.1126/science.288.5467.831>
- (13) Decharat, A., Yu, J., Boers, M., Stemme, G., & Niklaus, F. (2009). Room-temperature sealing of microcavities by cold metal welding. *Journal of Microelectromechanical Systems*, 18(6), 1318–1325. <http://doi.org/10.1109/JMEMS.2009.2030956>

ACADEMIC VITA

Michael Dexheimer

Education

Master of Science in Engineering Science

The Pennsylvania State University

Anticipated Graduation: *May 2019*

Bachelor of Science in Engineering Science

Schreyer Honors College

The Pennsylvania State University

Graduation: *Summer 2018*

Thesis Supervisor:

Dr. Huanyu Cheng

Work Experience

PPG Materials Research Institute Research Fellow – Dr. Huanyu Cheng – [2017 - Present]

Designed and executed experimental processes to improve transfer printing techniques. Manipulated mold geometries for the increased efficiency and effectiveness of the transfer printing process. Simulated material tests through finite element analysis that were later brought to fruition through CAD design and three-dimensional printing.

Undergraduate Research Assistant – Cheng Group, Dr. Huanyu Cheng – [2015 - Present]

Lead a group of students with similar interests in science, technology, and engineering to research future medical applications and the technological capabilities of transient electronic devices. Gained valuable research, communication, and leadership skills.

Undergraduate Research Assistant – Brain Develop. Lab, Dr. Rick Gilmore – [2015 - Present]

Investigated patterns of the brain and changes in behavior among both children and adults through the utilization of electroencephalogram and MRI imaging. Acquired experience in data collection and processing, as well as new insight in the research process as a whole.

CERI Undergraduate Research Experience –Magnetic Nanopaper, Penn State – [2016]

Inquired as to the current applications of magnetic nanopaper. Developed a research project through thorough literature review. Wrote and presented findings regarding the topic and developed plans for future projects.

Lab Technician, Penn State Hershey College of Med. – TCORS, Dr. Jonathon Foulds – [2016]

Responsible for the collection, processing, and organization of blood, urine and saliva samples. Acquired great knowledge regarding the research process across the sciences. Developed interpersonal skills through research participant interactions. Practiced molecular biology techniques through sample processing.

Awards:

Dean's List – *Every Semester in Attendance – Penn State, University Park*

Lyle W. and Virginia C. Coffey Scholarship in ESM – *Dep. Engineering Science and Mechanics. Received in the fall of 2016 “For excellent academic performance”.*

Gursahaney Fund for Excellence – *College of Engineering and Smeal College of Business. Received for academic excellence in participation in interdisciplinary coursework*

Memberships and Community Involvement:

Engineering Orientation Network – *Mentor*

Engineering Leadership Society – *Member*

ASME – *Member*

Phi Sigma Gama Honors Society – *Member*

2Days2Give Organization – *President*

American Cancer Soc. – *[2014 - Present]*

Summer Mathematics Tutor – *[2015-16]*

Religious Education Instruction – *[2012-16]*

Publications:

Review – J. Zhu, **M. Dexheimer**, H. Cheng, “Reconfigurable systems for multifunctional electronics,” *npj Flexible Electronics* (2017).

Presentations:

Abstract – RO. Gilmore, D. Farred, **M. Dexheimer**, A. Seisler, “The appearance and disappearance of visual forms defined by differential motion evokes distinctive EEG response in school-age children”, *Neuroscience* (2016)